

System size and energy dependence of the near-side of high- p_T triggered di-hadron correlations in STAR

Christine Nattrass for the STAR collaboration*

Yale University

E-mail: christine.nattrass@yale.edu

Previous studies have indicated that the near-side peak of high- p_T triggered di-hadron correlations can be decomposed into two parts, a jet-like correlation and the *Ridge*. We present data from Cu+Cu and Au+Au collisions at $\sqrt{s_{NN}} = 62$ GeV and 200 GeV, which should allow more robust tests of models. The jet-like correlation is narrow in both azimuth and pseudorapidity and has properties similar to those expected from vacuum fragmentation. The yield of particles in the jet-like correlation are presented for both systems and at both energies and compared to the yields expected from di-hadron correlations in PYTHIA 8.1. The *Ridge* is narrow in azimuth but broad in pseudorapidity and roughly independent of pseudorapidity within STAR's acceptance. Attempts have been made to explain the production of the *Ridge* component as coming from recombination, momentum kicks, Glasma flux tubes, and a plasma instability. However, few models have attempted to quantitatively calculate the characteristics of the *Ridge*. The yield in the *Ridge* is compared for all systems and energies. The implications for measurements at the LHC are discussed in context of the data and models.

High- p_T Physics at LHC -09

February 4- 7 2009

Prague, Czech Republic

*Speaker.

1. Introduction

Previous studies at RHIC demonstrated significant modification of the near-side peak of high- p_T triggered di-hadron correlations [1, 2]. The near-side can be decomposed into two components, a jet-like correlation and the *Ridge*. The jet-like correlation is similar to high- p_T triggered di-hadron correlations observed in $p + p$, $d + Au$, and PYTHIA. It is narrow in both azimuth and pseudorapidity and its particle composition is similar to the inclusive particle ratios in $p + p$ at the same collision energy and particle momenta [2, 3].

The *Ridge* is a novel feature not observed in $p + p$ and $d + Au$ collisions and not explained by simple models such as PYTHIA. STAR has done extensive studies of the properties of the *Ridge*; other relevant measurements are discussed in [4, 5]. Although this paper focuses on high- p_T triggered correlations, a "soft" *Ridge* has been observed by the STAR collaboration in untriggered correlations as well [6, 7]. Many mechanisms have been proposed for the production of the *Ridge* but there have been few quantitative comparisons with the data to date.

The momentum kick model assumes an initial distribution of medium partons which is roughly independent of pseudorapidity. Collisions with a hard parton create a correlation in azimuth between the hard parton and the medium partons [8]. Several mechanisms for the production of the *Ridge* involve hydrodynamics. One model explains the *Ridge* as resulting from a parton wind due to longitudinal flow [16]. It is also proposed that the *Ridge* arises due to a combination of a bias for the trigger to be near the surface of the medium and radial flow [17–19]. Recent calculations in a full hydrodynamical model also show a *Ridge* [15]. Several models explain the *Ridge* as a correlation in pseudorapidity created by plasma instabilities from fluctuations in strong fields early in the collision [9–14]. Some of these models are compared to the untriggered data, however, these models have been hypothesized to be able to explain the high- p_T triggered *Ridge* [13, 14]; these models also need radial flow to produce a *Ridge* large enough to be comparable to the data.

2. Analysis method

Data from the STAR detector from $Au + Au$ collisions at $\sqrt{s_{NN}} = 62$ GeV are from RHIC's fourth year run (2004) and data from $Cu + Cu$ collisions at $\sqrt{s_{NN}} = 62$ GeV and 200 GeV are from RHIC's fifth year run (2005.) Details of the STAR detector can be found in [20]. These data are compared to previous studies done in the $Au + Au$ data at $\sqrt{s_{NN}} = 200$ GeV from RHIC's fourth year run [2].

In a given event, a high- p_T track, called the trigger particle, is selected and the distribution of lower momentum particles, called associated particles, relative to that track in $\Delta\eta$ and $\Delta\phi$ is determined. Multiple tracks in a single event may be counted as trigger and associated particles. Since these measurements are limited by statistics and the data are symmetric about $\Delta\phi = 0$ and $\Delta\eta = 0$, the data are reflected about $\Delta\phi = 0$ and $\Delta\eta = 0$ to minimize statistical fluctuations. The single track efficiency is dependent on particle type, collision system and energy, p_T , and centrality and the correction for associated particles is applied on a track-by-track basis. The final distribution is normalized by the number of trigger particles, so no correction for the efficiency of reconstructing the trigger particle is necessary. Detector acceptance is corrected for by selecting a random trigger from the distribution of trigger particles in (ϕ, η) and mixing it with a random associated particle

from the distribution of associated particles in (ϕ, η) . This is done for each bin in p_T and centrality. This is used to calculate the correction for detector acceptance as a function of $(\Delta\phi, \Delta\eta)$. This is done for the full sample of events to give the average distribution of associated particles relative to a high- p_T trigger particle $\frac{1}{N_{trigger}} \frac{d^2N}{d\Delta\phi d\Delta\eta}$.

The *Ridge* was previously observed to be approximately independent of $\Delta\eta$ within the acceptance of the STAR TPC while the jet-like correlation is confined to $|\Delta\eta| < 0.75$ [1, 21]. This is used to separate the jet-like correlation and the *Ridge*. The yield, number of particles associated with each trigger particle within limits on $p_T^{associated}$ and $p_T^{trigger}$, is studied.

2.1 Determination of jet-like yield

To determine the jet-like yield, Y_{Jet} , the projection of the distribution of particles $\frac{d^2N}{d\Delta\phi d\Delta\eta}$ is taken in two different ranges in pseudorapidity:

$$\frac{dY_{ridge}}{d\Delta\phi} = \frac{1}{N_{trigger}} \int_{-1.75}^{-0.75} \frac{d^2N}{d\Delta\phi d\Delta\eta} d\Delta\eta + \frac{1}{N_{trigger}} \int_{0.75}^{1.75} \frac{d^2N}{d\Delta\phi d\Delta\eta} d\Delta\eta \quad (2.1)$$

$$\frac{dY_{jet+ridge}}{d\Delta\phi} = \frac{1}{N_{trigger}} \int_{-0.75}^{0.75} \frac{d^2N}{d\Delta\phi d\Delta\eta} d\Delta\eta \quad (2.2)$$

where the former contains only the *Ridge* and the latter contains both the jet-like correlation and the *Ridge*. The jet-like yield on the near-side is the integral over $-1 < \Delta\phi < 1$:

$$Y_{jet}^{\Delta\phi} = \int_{-1}^1 \left(\frac{dY_{jet+ridge}}{d\Delta\phi} - \frac{0.75}{1} \frac{dY_{ridge}}{d\Delta\phi} \right) d\Delta\phi. \quad (2.3)$$

The factor in front of the second term is the ratio of the $\Delta\eta$ width in the region containing the jet-like correlation and the *Ridge* to the width of the region containing only the *Ridge*. The Y_{Jet} is determined by fitting a Gaussian to the peak at $\Delta\phi \approx 0$ after subtracting the *Ridge*. Since the data have been reflected about $\Delta\phi = 0$ and $\Delta\eta = 0$, the projections in $\Delta\phi$ and $\Delta\eta$ and the bin counting are done over half of the range and then scaled up to ensure correct error propagation.

There is a slight loss of particles at small $(\Delta\phi, \Delta\eta)$ due to track merging. The correction for this effect is in progress. It affects only the jet-like correlation and leads to a loss of $\approx 10\%$ of the jet-like yield at the lowest $p_T^{trigger}$ in central $Au + Au$, where it is largest [22].

2.2 Determination of *Ridge* yield

There is a large combinatorial background which is dependent on $\Delta\phi$ given by

$$\frac{dY_{bgd}}{d\phi} = B(1 + 2\langle v_2^{trigger} \rangle \langle v_2^{associated} \rangle \cos(2\Delta\phi)) \quad (2.4)$$

where v_2 is the second order harmonic in a Fourier expansion of the momentum anisotropy relative to the reaction plane [23]. Systematic errors come from the errors on B , $\langle v_2^{trigger} \rangle$ and $\langle v_2^{associated} \rangle$. v_2 is determined from independent measurements. It is assumed that v_2 is the same at a given multiplicity for events with a trigger particle as for those without a trigger particle and that v_2 is

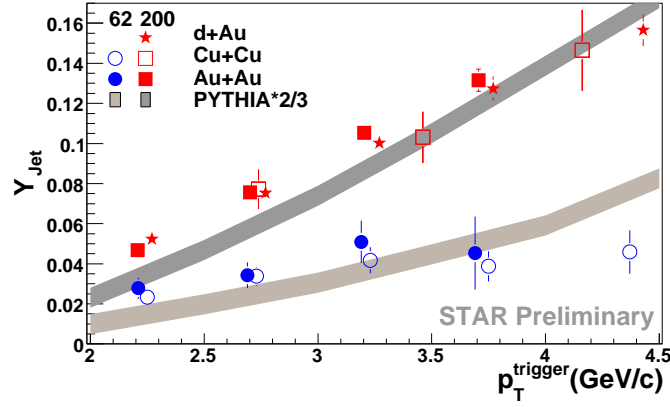


Figure 1: p_T^{trigger} dependence of the Y_{Jet} for $\text{Cu} + \text{Cu}$ and $\text{Au} + \text{Au}$ at $\sqrt{s_{\text{NN}}} = 62$ GeV and $d + \text{Au}$, $\text{Cu} + \text{Cu}$, and $\text{Au} + \text{Au}$ at $\sqrt{s_{\text{NN}}} = 200$ GeV for $1.5 \text{ GeV}/c < p_T^{\text{associated}} < p_T^{\text{trigger}}$ compared to the yield from PYTHIA scaled by 2/3.

independent of η , a reasonable assumption within the acceptance of the STAR TPC based on the available data [24, 25]. For each data set $v_2(p_T)$ was fit to the measured data for each centrality bin to determine $\langle v_2^{\text{trigger}} \rangle$ and $\langle v_2^{\text{associated}} \rangle$. Details of the v_2 subtraction are given in [2] for $\text{Au} + \text{Au}$ collisions at $\sqrt{s_{\text{NN}}} = 200$ GeV and in [21] for $\text{Cu} + \text{Cu}$ collisions at $\sqrt{s_{\text{NN}}} = 200$ GeV. For $\text{Cu} + \text{Cu}$ collisions at $\sqrt{s_{\text{NN}}} = 62$ GeV, v_2 using the reaction plane as determined from tracks in the Forward Time Projection Chamber was used as the nominal value and the lower bound was determined from a multiplicity-dependent approximation as described for $\sqrt{s_{\text{NN}}} = 200$ GeV in [21]. v_2 and its systematic errors were taken from [26] for $\text{Au} + \text{Au}$ collisions at $\sqrt{s_{\text{NN}}} = 62$ GeV. B is determined using the Zero Yield At Minimum (ZYAM) method [27].

To determine the yield of the *Ridge*, Y_{Ridge} , the di-hadron correlation $\frac{d^2N}{d\Delta\phi d\Delta\eta}$ is projected over the entire $\Delta\eta$ region. To minimize the effects of statistical fluctuations in the determination of the background, $\frac{dY_{\text{bgd}}}{d\phi}$, Y_{Jet} is subtracted after the projection in $\Delta\eta$:

$$Y_{\text{Ridge}} = 1/N_{\text{trigger}} \int_{-1.75}^{1.75} \int_{-1}^1 \left(\frac{d^2N}{d\Delta\phi d\Delta\eta} - \frac{dY_{\text{bgd}}}{d\phi} \right) d\Delta\phi d\Delta\eta - Y_{\text{Jet}}^{\Delta\eta}. \quad (2.5)$$

The integration over $\Delta\phi$ is done fitting a Gaussian to the peak around $\Delta\phi \approx 0$.

3. Results

3.1 The jet-like correlation

Fig. 1 shows the Y_{Jet} as a function of p_T^{trigger} for $\text{Cu} + \text{Cu}$ and $\text{Au} + \text{Au}$ at $\sqrt{s_{\text{NN}}} = 62$ GeV and $d + \text{Au}$, $\text{Cu} + \text{Cu}$, and $\text{Au} + \text{Au}$ at $\sqrt{s_{\text{NN}}} = 200$ GeV. For a given collision energy, there is no difference within statistical errors between the different collision systems. This would be expected if the jet-like correlation is dominantly produced from vacuum fragmentation. These data are compared to the charged particle yields expected from PYTHIA 8.1 using the default settings [28],

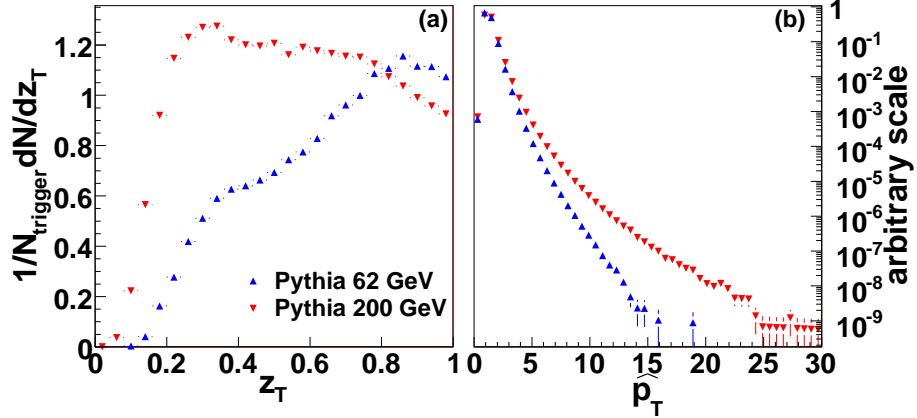


Figure 2: (a) distribution of trigger particles z_T and (b) \hat{p}_T distribution in PYTHIA at $\sqrt{s_{NN}} = 62$ GeV from PYTHIA 8.1 for $1.5 \text{ GeV}/c < p_T^{\text{associated}} < p_T^{\text{trigger}}$ and $3.0 < p_T^{\text{trigger}} < 6.0 \text{ GeV}/c$ at $\sqrt{s_{NN}} = 62$ GeV and $\sqrt{s_{NN}} = 200$ GeV.

scaled by 2/3. Although the yield is off by a factor of 2/3, the shape of the p_T^{trigger} dependence is described well by PYTHIA.

The difference between $\sqrt{s_{NN}} = 62$ GeV and 200 GeV is also described well by PYTHIA. Fig. 2(a) shows the $z_T = p_T/\hat{p}_T$ distribution in PYTHIA and Fig. 2(b) shows the distribution of \hat{p}_T , the momentum transfer of the hard scattering, at both energies. The \hat{p}_T is the parameter in PYTHIA for the transverse momentum in the hard subprocess [28]. For the same p_T^{trigger} , a higher average z_T is selected in collisions at $\sqrt{s_{NN}} = 62$ GeV, meaning that the trigger particle takes a greater percentage of the energy. The slope of \hat{p}_T is considerably steeper in $\sqrt{s_{NN}} = 62$ GeV than in $\sqrt{s_{NN}} = 200$ GeV so for a fixed p_T^{trigger} the trigger particle is more likely to have come from a lower energy parton. The large difference between Y_{Jet} at $\sqrt{s_{NN}} = 62$ GeV and 200 GeV can then be understood as arising from the difference in the underlying jet spectra which lead to the di-hadron correlations.

The $p_T^{\text{associated}}$ dependence of Y_{Jet} is shown in Fig. 3 for $\text{Cu} + \text{Cu}$ and $\text{Au} + \text{Au}$ at $\sqrt{s_{NN}} = 62$ GeV and $d + \text{Au}$, $\text{Cu} + \text{Cu}$, and $\text{Au} + \text{Au}$ at $\sqrt{s_{NN}} = 200$ GeV compared to the yield from PYTHIA scaled by 2/3. The inverse slope parameters from fits of the data are given in Table 1. The data for $\text{Cu} + \text{Cu}$ and $\text{Au} + \text{Au}$ collisions are within errors at a given collision energy. PYTHIA overestimates the inverse slope parameter of the spectra of particles in the jet-like correlation for collisions at $\sqrt{s_{NN}} = 62$ GeV.

Y_{Jet} as a function of N_{part} is shown in Fig. 4. At a given N_{part} , the data in $\text{Cu} + \text{Cu}$ and $\text{Au} + \text{Au}$ collisions are within errors at both $\sqrt{s_{NN}} = 62$ GeV and $\sqrt{s_{NN}} = 200$ GeV. There is a slight increase with N_{part} from $d + \text{Au}$ to central $\text{Au} + \text{Au}$. This increase may either be a slight modification of the jet-like correlation or be a misidentification of part of the *Ridge* into the jet-like correlation because of the inherent assumption in the method for determining the yield that the *Ridge* is independent of pseudorapidity.

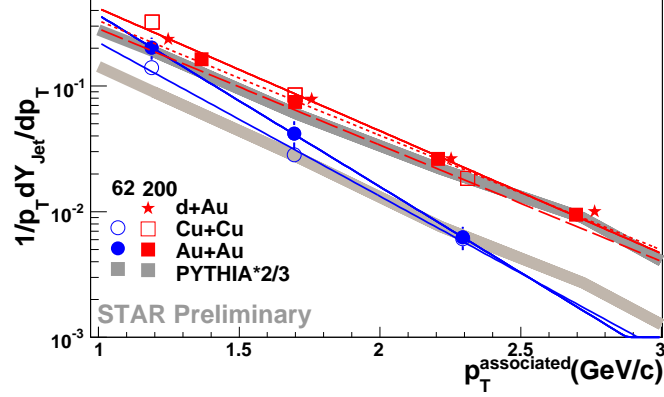


Figure 3: $p_T^{\text{associated}}$ dependence of Y_{Jet} for $\text{Cu} + \text{Cu}$ and $\text{Au} + \text{Au}$ at $\sqrt{s_{NN}} = 62$ GeV and $d + \text{Au}$, $\text{Cu} + \text{Cu}$, and $\text{Au} + \text{Au}$ at $\sqrt{s_{NN}} = 200$ GeV for $3.0 < p_T^{\text{trigger}} < 6.0$ GeV/c compared to the yield from PYTHIA scaled by 2/3. The inverse slope parameters from fits of an exponential to data and to PYTHIA are given in Table 1.

Table 1: Inverse slope parameter k (MeV/c) of $p_T^{\text{associated}}$ for fits of data in Table 1 to $Ae^{-p_T/k}$. The inverse slope parameter for inclusive π^- are from a fit to the data in [29] as a function of p_T above 1.0 GeV/c. Statistical errors only.

	$\sqrt{s_{NN}} = 62$ GeV h-h	$\sqrt{s_{NN}} = 200$ GeV h-h
<i>Au Ridge</i>		438 ± 4
<i>Au + Au jet-like correlation</i>	317 ± 26	478 ± 8
<i>Cu + Cu jet-like correlation</i>	355 ± 21	445 ± 20
<i>d + Au jet-like correlation</i>		469 ± 8
PYTHIA	424 ± 5	473 ± 3
Inclusive π^-	280.9 ± 0.4	330.9 ± 0.3

3.2 The Ridge

The *Ridge* yield as a function of N_{part} is shown in Fig. 5. At a given N_{part} , the data from $\text{Cu} + \text{Cu}$ and $\text{Au} + \text{Au}$ collisions at the same collision energy are within errors. The *Ridge* yield is considerably smaller in collisions at $\sqrt{s_{NN}} = 62$ GeV than those at $\sqrt{s_{NN}} = 200$ GeV, just like the jet-like yield. An interesting trend is observed for the *Ridge* yield; Fig. 6 shows that the ratio of the *Ridge* yield to the jet-like yield as a function of N_{part} for both energies is the same.

4. Discussion and implications for the LHC

The data imply that the jet-like correlation is produced dominantly by fragmentation. No collision system dependence is observed. Y_{Jet} increases slightly as a function of N_{part} ; this may come from slight modification of the jet-like correlation in $A + A$ collisions or it may be an artifact of the method for separating the jet-like correlation and the *Ridge*. PYTHIA describes the shape

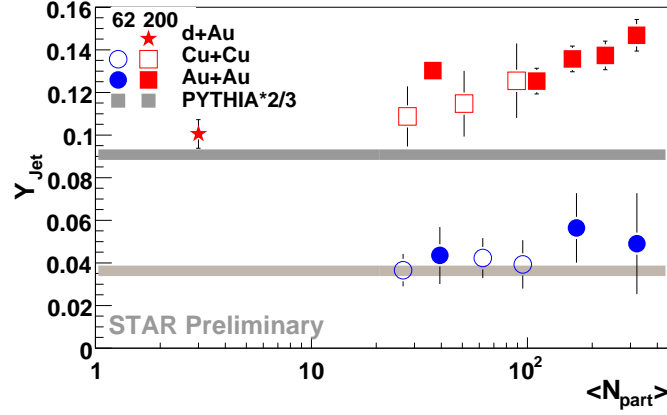


Figure 4: N_{part} dependence of the Y_{jet} for $Cu + Cu$ and $Au + Au$ at $\sqrt{s_{NN}} = 62$ GeV and $d + Au$, $Cu + Cu$, and $Au + Au$ at $\sqrt{s_{NN}} = 200$ GeV for $3.0 < p_T^{trigger} < 6.0$ GeV/c and 1.5 GeV/c $< p_T^{associated} < p_T^{trigger}$ compared to the yield from PYTHIA.

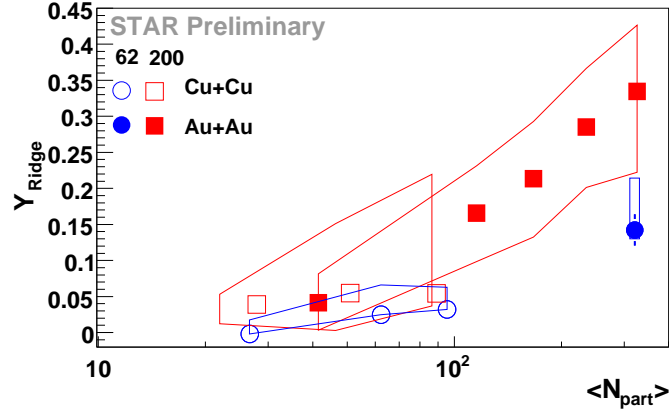


Figure 5: Y_{Ridge} dependence on N_{part} for $\sqrt{s_{NN}} = 62$ GeV and $\sqrt{s_{NN}} = 200$ GeV for $3.0 < p_T^{trigger} < 6.0$ GeV/c and 1.5 GeV/c $< p_T^{associated} < p_T^{trigger}$.

of the $p_T^{trigger}$ and collision energy dependence of the jet-like correlation well, implying that the shape of the $p_T^{trigger}$ and $p_T^{associated}$ dependence is dominated by the kinematic cuts on $p_T^{associated}$ and $p_T^{trigger}$. This means that simple models such as PYTHIA can be used to understand the effects of the kinematic cuts on the distribution of jet energies which lead to the jet-like correlation, providing insight into measurement of the *Ridge*.

Most models for the *Ridge* would qualitatively predict a *Ridge* at the LHC, however, few quantitative descriptions of the energy dependence of the *Ridge* have been made. The Momentum Kick model can describe the energy dependence of the data at RHIC [30]. Plasma instability models would also predict a *Ridge*, however, few quantitative comparisons of the models to the data have been done and there have been no attempts at describing the collision energy dependence [9–14]. Models dependent on hydrodynamics [15–17] would also predict a *Ridge* at the LHC, however, no quantitative predictions have been made. If collective flow is larger at the LHC, the *Ridge* would

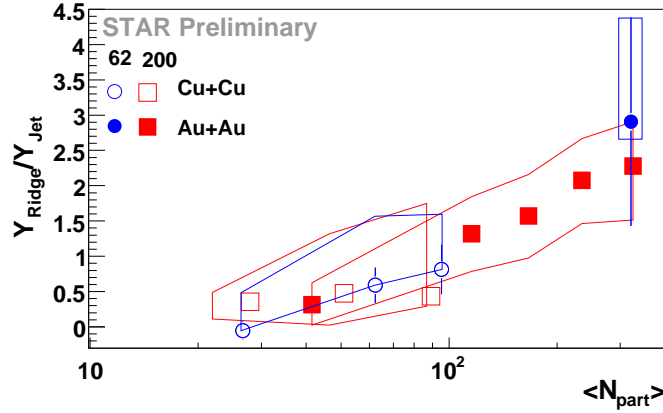


Figure 6: Y_{Ridge}/Y_{Jet} dependence on N_{part} for $\sqrt{s_{NN}} = 62$ GeV and $\sqrt{s_{NN}} = 200$ GeV for $3.0 < p_T^{trigger} < 6.0$ GeV/c and $1.5 \text{ GeV/c} < p_T^{associated} < p_T^{trigger}$.

also be expected to be bigger.

A straightforward extrapolation from the data at RHIC can provide estimates for the expectations for measurements of the *Ridge* at the LHC. Fig. 6 showed that, at least for the kinematic cuts used in these studies, the Y_{Ridge}/Y_{Jet} ratio is the same for collisions at $\sqrt{s_{NN}} = 62$ GeV and $\sqrt{s_{NN}} = 200$ GeV. If this is also true at LHC energies, the Y_{Ridge}/Y_{Jet} ratio will be the same for the same kinematic cuts. The combinatorial background will be much larger at 5.5 TeV for $1.5 \text{ GeV/c} < p_T^{associated} < p_T^{trigger}$ and $3.0 < p_T^{trigger} < 6.0$ GeV/c the dominant systematic error at RHIC is due to v_2 subtraction, so measurements of the *Ridge* for the same kinematic cuts may be difficult if v_2 at the LHC is comparable to that at RHIC. The combinatorial background can be reduced by increasing $p_T^{trigger}$ and $p_T^{associated}$. Fig. 1 shows that Y_{Jet} increases rapidly with $p_T^{trigger}$. Y_{Ridge} is roughly independent of $p_T^{trigger}$ [1]. This means that increasing $p_T^{trigger}$ decreases Y_{Ridge}/Y_{Jet} . It was shown in [1] that the spectrum of particles in the *Ridge* is softer than those in Y_{Jet} . This means that increasing $p_T^{trigger}$ will also decrease Y_{Ridge}/Y_{Jet} . Measurements of the *Ridge* at the LHC may be difficult because of the large combinatorial background if these naive extrapolations of RHIC data are correct.

5. Conclusions

Measurements at RHIC imply that the jet-like correlation is dominantly produced by vacuum fragmentation. There have been numerous measurements of the *Ridge* and many production mechanisms have been proposed, however, there have been few quantitative comparisons with the data. Both the data and models imply that the *Ridge* should be present at the LHC. With additional theoretical insight on the collision energy dependence of the *Ridge*, these measurements should be able to provide a better understanding of the origin of the *Ridge*.

References

- [1] J. Putschke (STAR), J. Phys. G **34**, 679-683 (2007) [nucl-ex/0701074].

- [2] J. Bielcikova (STAR), J. Phys. G **34**, 929-932 (2007) [nucl-ex/0701047]
- [3] C. Suarez (STAR), Quark Matter 2008, unpublished
- [4] J. Bielcikova (STAR), these proceedings
- [5] O. Barannikova, these proceedings
- [6] J. Adams et al, Phys. Rev. C **73**, 64907 (2006) [nucl-ex/0411003]
- [7] M. Daugherty, J. Phys. G **35**, 104090 (2008) [nucl-ex/0806.2121]
- [8] C. Y. Wong, Phys. Rev. C **76**, 054908 (2007) [hep-ph/0707.2385]
- [9] A. Dumitru, Y. Nara, B. Schenke, M. Strickland, Phys.Rev.C **78** 024909 (2008) [hep-ph/0710.1223]
- [10] A. Majumder, B. Muller, S. Bass, Phys.Rev.Lett. **99** 042301 (2007) [hep-ph/0611135v2]
- [11] P. Romatschke, Phys. Rev. C **75** 014901 (2007) [hep-ph/0607327]
- [12] R. Mizukawa, T. Hirano, M. Isse, Y. Nara, A. Ohnishi, J.Phys.G **35** 104083 (2008) [nucl-th/0805.2795]
- [13] A. Dumitru, F. Gelis, L. McLerran, R. Venugopalan, Nucl. Phys. A **810** 91,(2008) [hep-ph/0804.3858]
- [14] S. Gavin, L. McLerran, G. Moschelli [nucl-th/0806.4718]
- [15] J. Takahashi, B.M. Tavares, W.L.Qian, F. Grassi, Y. Hama, T. Kodama, N. Xu [nucl-th/0902.4870]
- [16] N. Armesto, C. Salgado, U. Wiedemann, Phys. Rev. C **72**, 064910 (2005) [hep-ph/0411341]
- [17] S. Voloshin, Phys. Rev. B **632**, 490 (2006) [nucl-ex/0902.0581]
- [18] C. A. Pruneau, S. Gavin, S. A. Voloshin, Nucl.Phys.A **802** 107-121 (2008) [nucl-ex/0711.1991]
- [19] E. Shuryak, Phys.Rev.C **76** 047901 (2007) [nucl-th/0706.3531]
- [20] K. H. Ackermann *et al* , Nucl. Inst. Meth. A **499**, 624 (2003)
- [21] Nattrass C (STAR), J. Phys. G **35**, 044063 (2008) [nucl-ex/0804.4558]
- [22] M. Bombara (STAR), J. Phys. G **35**, 044065 (2008)
- [23] J.Bielcikova, S.Esumi, K.Filimonov, S.Voloshin, J.P.Wurm, Phys.Rev. C **69** 021901 (2004) [nucl-ex/0311007]
- [24] Back B B *et al* , Phys. Rev. C **72** 051901 (2005) [nucl-ex/0407012]
- [25] Back B B *et al* , Phys. Rev. Lett. **94** 122303 (2005) [nucl-ex/0406021]
- [26] B. I. Abelev *et al* (STAR), Phys. Rev. C **75**, 54906 (2007) [nucl-ex/0701010]
- [27] Adams J *et al* (STAR) Phys. Rev. Lett. **95** 152301 (2005) [nucl-ex/0501016]
- [28] T. Sjöstrand, S. Mrenna, P. Skands, Comput.Phys.Commun. **178** 852-867 (2008) [hep-ph/0710.3820]
- [29] B. I. Abelev *et al* (STAR), Phys. Lett. **B655**, 104 (2007)
- [30] C. Y. Wong, Phys.Rev.C **78** 064905 (2008) [hep-ph/0806.2154]